ELSEVIER

Journal of Chromatography A, 695 (1995) 175–183

JOURNAL OF CHROMATOGRAPHY A

Near-infrared laser-induced fluorescence detection in column liquid chromatography. A comparison of various lasers and detection systems
II☆. Pulsed lasers

A.J.G. Mank*, N.H. Velthorst, U.A. Th. Brinkman, C. Gooijer

Department of General and Analytical Chemistry, Free University, De Boelelaan 1083, 1081 HV Amsterdam, Netherlands

First received 21 June 1994; revised manuscript received 2 December 1994

Abstract

The applicability of two pulsed lasers, a XeCl-excimer/dye laser and a Nd:YAG/dye laser combination, as excitation sources for near-infrared (NIR) laser-induced fluorescence (LIF) detection in column liquid chromatography (LC) is studied. Using gradient LC, the best detection limit for the model compound, disulphonated aluminum phthalocyanine (AlPcS2), is $4 \cdot 10^{-12}$ *M* obtained using the excimer/dye laser combination. This value is about 10-fold lower than obtained with the Nd:YAG laser, but 20-fold higher than for CW diode laser excitation, as reported in Part I of this study [*J. Chromatogr. A*, 695 (1995) 175]. Because of excitation saturation the optimum results were obtained using only a fraction of the available power. A detailed theoretical discussion is presented which underlines the experimental results and provides insight into the factors that determine the detection limits.

1. Introduction

In Part I of this study [1] the performance of continuous wave (CW) laser systems in near-infrared laser-induced fluorescence (NIR LIF) detection applied to conventional-size column liquid chromatography (LC) was studied, using gradient LC of disulphonated aluminum phthalocyanine (AlPcS2) as a model system. The present paper is devoted to pulsed lasers, i.e. the frequency-doubled Nd:YAG laser and the XeCl-excimer laser, both combined with dye lasers. Such lasers have rarely been used for detection in LC. In principle, they might be interesting because they are readily tunable not only in the visible but also (by utilizing frequency doubling techniques) in the UV part of the spectrum. Selectivity enhancement by the introduction of time-resolution has little potential because fluorescence lifetimes of most analytes in liquid solutions are close to or even shorter than the pulse duration; the fluorescence lifetime of AlPcS2 is 5 to 6 ns [2].

Compared with CW lasers, pulsed lasers exhibit some special features in fluorescence detection. Because of their extremely high peak powers, both excitation saturation and photo-

* Corresponding author.

☆ For Part I see Ref. [1].

0021-9673/95/$09.50
SSDI 0021-9673(94)01196-6

chemical decomposition of analytes are expected to play a role. The influence of pulse duration, repetition rate and average power has to be quantified together with the role of pulse-to-pulse fluctuations.

2. Experimental

2.1 Chemicals, chromatography, detection

Chemicals, LC instrumentation, general aspects of detection (cell construction, emission collection and NIR light detection) have been described in Part I [1]. For signal processing boxcar integration was used.

Boxcar integration

Two Stanford Research (Palo Alto, CA, USA) SR250 boxcar integrators were used to monitor the fluorescence and the reference signals. A Stanford Research SR235 analog processor unit transforms the voltage readout to a signal that is handled by a Stanford Research SR245 Computer Interface. Data are sent to a Macintosh SE computer and transformed to ASCII with a home-made program. Both channels can be used at the same time, allowing ratioing of the data in Igor (WaveMetrics, Lake Oswego, OR, USA).

To supply the boxcar channels with a trigger pulse, about 5% of the excitation light is directed towards a BPW 28 picosecond photodiode. For time-resolved detection a DB463 delay box (EG and G Ortec, Oak Ridge, TN, USA) is applied to optimize the delay. A gatewidth of 60 ns is used for fluorescence detection, starting 5 ns before the laser pulse reaches the flow cell because of the short fluorescence lifetime of the model compound.

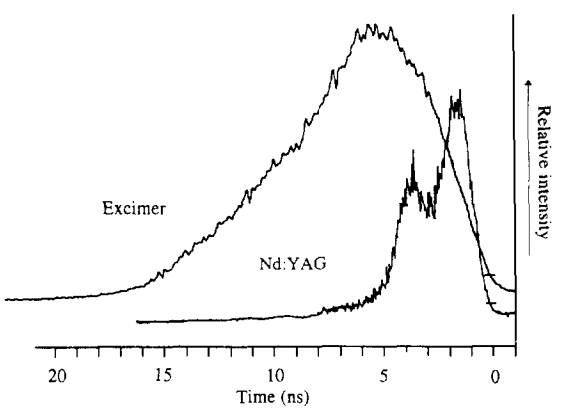

Fig. 1. Pulse shape for the Nd:YAG/dye laser combination and the excimer/dye laser combination, measured with a Siemens (München, Germany) BPW28 fast photodiode and a Tektronix (Beaverton, OR, USA) TDS50 two-channel digitizing oscilloscope.

2.2 Laser systems

The excimer/dye laser and the Nd:YAG/dye laser combination will be denoted without specifying the dye laser. Their pulse shapes are depicted in Fig. 1.

Nd:YAG laser

A YG580 Quantel frequency-doubled Nd:YAG laser is used in combination with an Oxazine 170-dye laser (TDL50), which delivers 16 mW at 670 nm with a repetition frequency of 10 Hz. With an average pulse length of 6 ns (Fig. 1), a peak power of about $2.7 \cdot 10^5$ W is available. Pulse-to-pulse fluctuations are 20% on average. Signals were averaged over 1 s (10 pulses) before further processing.

Excimer laser

A Lambda Physic Model LPX101i XeCl-excimer laser is used in combination with a Model LPD3000 DCM-dye laser, which delivers 250 mW at 670 nm with a repetition rate of 100 Hz. With an average pulse length of 15 ns (Fig. 1), this corresponds with a peak power of $1.7 \cdot 10^5$ W. Pulse-to-pulse fluctuations are 3% on average.

If required, the excitation power was reduced with standard neutral density filters. Signals were averaged over 1 s (100 pulses) before further processing.

3. Results and discussion

Pulsed lasers provide extremely high irradiances because the radiation energy is delivered during very short periods of time. As a result, apart from possible detector damage occurring at irradiances higher than $1 \cdot 10^8$ W cm^{-2}, saturation effects and photodestruction have to be taken into account. Two aspects will be discussed here, i.e. the degree of saturation during the laser pulses and the experimental optimization of NIR LIF detection.

At the excitation wavelength used (670 nm), the molar absorptivity, ϵ, of AlPcS2 is as large as 180 000 l mol^{-1} cm^{-1}. The absorption rate constant, k_a, can be calculated [3] from Eqn. 1:

$$k_a = 3.8 \cdot 10^{-21} \epsilon I, \quad (1)$$

where I is the incident light intensity (photons cm^{-2} s^{-1}). I is related to the average power of the laser (P in J s^{-1}), the laser beam cross section (D in cm^2), the emitted wavelength (λ in m), the Planck constant (h in J s) and the light velocity (c in m s^{-1}) according to:

$$I = (P\lambda)/(Dhc) \quad (2)$$

For simplicity, a uniform distribution of the laser light intensity over a circular cross section of the laser beam is assumed. Confining our attention to the Nd:YAG/dye laser combination operated at 670 nm, during a laser pulse (1.6 mJ, 6 ns) $5.3 \cdot 10^{15}$ photons pass through the flow cell. Using a circular beam with a diameter of 500 μm, this corresponds with an incident light intensity of $4.5 \cdot 0^{26}$ photons cm^{-2} s^{-1} and a k_a of $3 \cdot 10^{11}$ s^{-1}.

It is readily seen that under such efficient excitation conditions ground-state depletion (excitation saturation) will be complete after a time interval which is much shorter than the pulse length, since return to the ground state within this time is negligible. Assuming first-order kinetics, the relative number of molecules left in the ground state, $[A]/[A_0]$, after a certain excitation time, t, can be written as:

$$[A]/[A_0] = e^{-k_a t} \quad (3)$$

This implies that for $k_a = 3 \cdot 10^{11}$ s^{-1}, 99% of the molecules is excited within 0.1 ns. Of course, at lower irradiances the depletion process will be less rapid. Nevertheless, even if only 0.1% of the available laser power is used so that k_a is 1,000-fold lower, the role of saturation is obvious: less than 15% of the molecules will be left in the ground state at the end of the pulse. In other words, not even the use of only 0.1% of the available power will result in a noticeable loss of signal intensity. In fact, at lower irradiances, detectability will be improved, since scatter background is strongly reduced. Using the same approach it can be shown that the same is true for the excimer/dye laser combination that is examined in this study.

Of course, for laser pulses longer than the fluorescence lifetime of the analyte, the number of analyte molecules that is actually in the excited state during the laser pulse is strongly influenced by the simultaneous return of the molecules to the ground state. Therefore, Eqn. 3 can not be used for quantitative calculations. A more thorough treatment is required to obtain a reliable estimate of the number of photons that is emitted by a single molecule passing through the laser beam. This topic is discussed in the Appendix and applied to the excitation conditions at which the maximum signal-to-noise ratio (S/N ratio) is obtained for the two pulsed lasers examined. In section 3.4 the experimental detection limits obtained will be compared with those calculated in the Appendix.

For the Nd:YAG and the excimer laser the experimental optimization of NIR LIF detection was performed as follows.

3.1. Nd:YAG laser

The Nd:YAG/dye laser combination emits 1.6 mJ per pulse of 6 ns, so that the irradiance is $1.2 \cdot 10^8$ W cm^{-2} if the laser beam is collimated to a diameter of 500 μm. Because of the low pulse repetition rate (10 Hz) a substantial fraction of the sample passing through the detector flow cell will not be irradiated at all. Between two consecutive pulses (time interval, 0.1 s) at a

flow rate of 1 ml min^{-1}, 1.7 μl of eluent passes through the cell. Consequently, with an irradiated volume of only 0.2 μl (flow cell diameter, 1.1 mm; beam diameter, 500 μm), less than 12% of all molecules will be excited. The importance of saturation is obvious: multiple excitation of a particular analyte molecule within one laser pulse will hardly occur, since the fluorescence lifetime of AlPcS2 is 5–6 ns (similar to the laser pulse duration); by far the larger fraction of the molecules will only be excited once (cf. Appendix). It should be noted that excitation of molecules residing in the excited state is a real possibility and might result in enhanced photodestruction compared to steady-state conditions under which a normal population distribution is maintained.

Experiments with neutral density filters inserted in the excitation beam were performed to find the actual dependence of signal and background noise on laser power (see Fig. 2A). Excitation saturation is already observed at 1% transmission of the laser light, whereas the background noise (before ratioing) increases more or less linearly over the whole power range studied. Ratioing reduced the noise significantly, especially if higher excitation power is used and shot noise is less important. Fig. 2B shows the *S/N* ratio over the same power range. Maximum *S/N* is obtained at only 0.5% of the available laser power, which corresponds with 0.08 mW average power. Ratioing (after data collection) with a 30-fold higher reference signal (Fig. 3A) enhances the *S/N* ratio about 2.5-fold: the detection limit of AlPcS2, calculated from the LC chromatograms of Fig. 3, improves from $1 \cdot 10^{-10}$ *M* (Fig. 3B) to $4 \cdot 10^{-11}$ *M* (Fig. 3C).

The above result is not unexpected since pulse-to-pulse fluctuations of the Nd:YAG laser are significant while its repetition frequency is low. The resulting flicker noise is about 20% of the background signal (see Fig. 3A). This background signal is 2-fold higher than expected if only Raman scatter were present (see ref. 1). Apparently elastically scattered light is not completely removed, a supposition that is supported by the relatively small increase in background

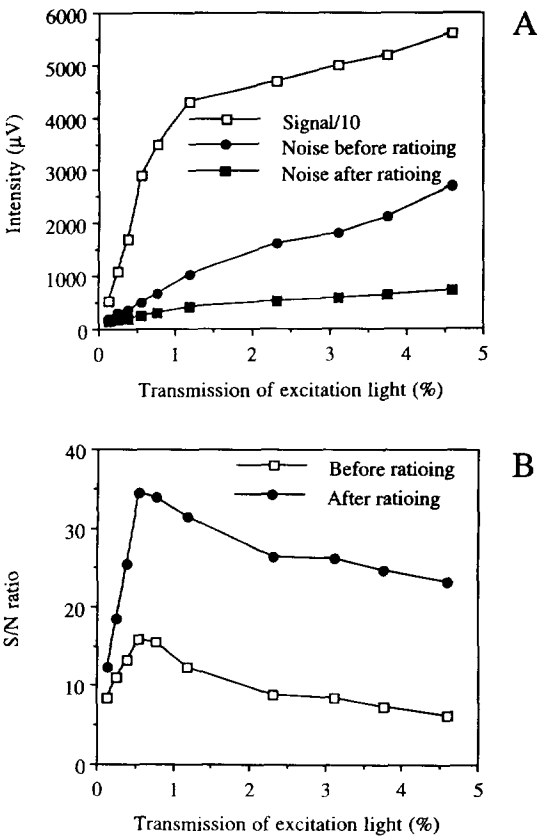

Fig. 2. Signal and background noise (A) and *S/N* ratio (B) as a function of the excitation power for the Nd:YAG laser.

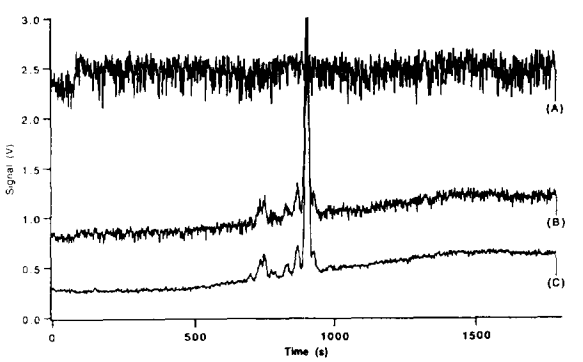

Fig. 3. LC chromatogram of $5 \cdot 10^{-10}$ *M* AlPcS2, recorded with the detection system using a Nd:YAG laser: (A) reference signal, divided by 10 to fit the scale; (B) fluorescence signal and (C) ratioed fluorescence signal, obtained by taking [(B)/(A)·2.5 V] − 0.5 V.

during LC gradient elution. Ratioing with the 30-fold higher reference signal efficiently removes the flicker noise from the chromatogram.

3.2. Excimer laser

Compared with the Nd:YAG laser, the excimer laser has a higher repetition rate, a longer pulse duration and less pulse-to-pulse fluctuations. At a repetition rate of 100 Hz, only 0.17 μl of sample passes the detector flow cell in the time interval between two consecutive pulses. In other words, all analyte molecules passing through the cell will be irradiated, but only very few will be excited by two consecutive laser pulses. Since the pulse is about 3 times longer (Fig. 1), multiple (2–3 times) excitation of a single analyte molecule is possible. The influence of pulse-to-pulse fluctuations (3%) is reduced to 0.3% if averaging is performed over 1 s or 100 pulses. This low value explains why in Fig. 4A the noise intensity increases with the square root of the laser power, indicating the predominance of shot noise. Thus, ratioing has no beneficial effect (Fig. 4B).

In view of the results obtained with the Nd:YAG laser, the excitation power was reduced to 20 mW with neutral density filters. Maximum *S/N* ratios are obtained at 5–7.5% of the available 20 mW (i.e. about 1.5 mW average) power (Fig. 4B). The detection limit for AlPcS2 is $4 \cdot 10^{-12}$ *M*.

Defocusing of the laser beam might result in better detection limits. However, increasing the beam diameter to 750 μm resulted in more scatter from the internal surface of the flow cell (1.1 mm bore). More importantly, the relative amount of flicker noise increased significantly, because spatial fluctuations in the beam resulted in variations in the amount of scatter from the eluent/silica interface inside of the flow cell. As a result, no gain in sensitivity is observed upon increasing the beam diameter.

Photochemical decomposition

The degree of decomposition depends on the chemical structure of the particular analyte, the

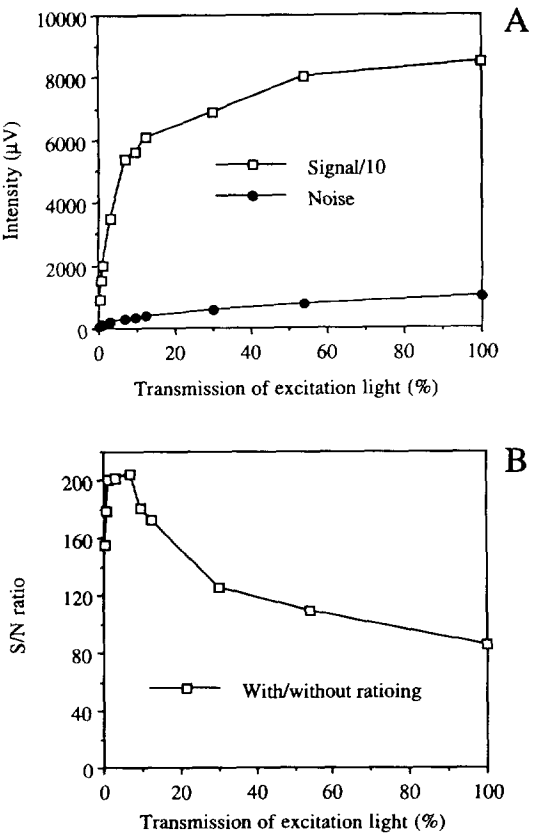

Fig. 4. Signal and background noise (A) and *S/N* ratio (B) as a function of the excitation power for the XeCl-excimer laser.

LC eluent flow rate and its composition [4]. Using flow injection of 1 ml of a $1 \cdot 10^{-10}$ *M* solution of AlPcS2 (excited at 1 mW average power), the signal height was independent of the flow rate over the range of 0.01–1 ml min^{-1}. At a flow rate of 0.01 ml min^{-1} any molecule can be excited at least 20 times by consecutive pulses of the excimer laser. This indicates that photodestruction of the present model compound is of minor importance, which is in line with the fact that phthalocyanines generally show high photostability [5]. One might argue that under steady-state conditions 20 excitations is rather limited [6], but here further excitation of excited molecules is a real possibility, which may result in

molecules that are more reactive than ground state molecules.

3.3. Experimental comparison

Obviously, the excimer laser is to be preferred over the Nd:YAG laser. Because of its higher repetition rate (100 Hz), the XeCl-excimer laser can excite all molecules in the present LC system. Furthermore, because of its longer pulse duration, the number of excitations per molecule within one pulse is in favour of the excimer laser. As a result, the optimum average excitation power for the XeCl-excimer laser is 15-fold higher than for the Nd:YAG laser: 1.4 mW and 0.08 mW, respectively.

3.4. Comparison with theory

The experimental differences in detection limits for the two pulsed lasers can be discussed theoretically. In the Appendix, the number of photons emitted per molecule in a flowing sample, n_f, after excitation with these lasers is calculated using an increment method. Under optimum experimental excitation conditions, n_f equals 0.4 for the Nd:YAG laser and 0.6 for the excimer laser, if the triplet state quantum yield (Q_T) of 0.33 is taken into account. Since excitation of a molecule by consecutive pulses can be neglected, the relative number of emitted photons s^{-1} is obtained by simply multiplying n_f with the repetition rate of the laser, giving 4.0 and 61, respectively (Table 1); theoretically 7740 photons s^{-1} are produced upon excitation with a 10 mW 670 nm CW diode laser (cf. Ref. [1]).

Obviously, the differences in background have to be considered as well. A major part of the background signal, n_b, is caused by Raman scatter, which does not show saturation and is proportional to the average laser power. The backgrounds observed for the diode laser and the excimer laser were 40 000 and 5600 photons s^{-1}, respectively. For the Nd:YAG laser, the background of 1400 photons s^{-1} probably contains some elastically scattered light in addition to Raman scatter. The remaining peak-to-peak noise on these backgrounds, completely determined by shot noise, is given in Table 1. Ratioing was performed if necessary to remove flicker noise. Dividing the relative signal (photons s^{-1}) by the peak-to-peak noise yields the relative S/N ratio (Table 1). Experimentally, the detection limits for the three laser systems stand as 1:20:200 (Table 2). For $Q_T = 0.33$, the corresponding calculated proportionality is 1:50:360, while for $Q_T = 0$ the proportionality is 1:30:250. Clearly, the high triplet yield for the model analyte favours the use of CW lasers.

In view of the simplifications introduced during the calculations, the results are satisfying: the theoretical and the experimental values show the

Table 1
Theoretical values for the relative NIR fluorescence signal height and noise amplitude upon excitation of AlPcS2 with different sources of laser light

Parameter	Diode laser	Excimer laser	Nd:YAG laser
Average power (mW)	10	1.4	0.08
Cross section beam (cm^2)	$1.0 \cdot 10^{-3}$	$2.5 \cdot 10^{-3}$	$2.5 \cdot 10^{-3}$
Repetition rate (Hz)	–	100	10
Relative signal (photons s^{-1})	7740 (7740)[a]	107 (61)[a]	6.0 (4.0)[a]
Peak-to-peak noise (photons s^{-1})[b]	800	300	150
Relative S/N ratio	9.7	0.36 (0.20)	0.040 (0.027)

[a] In parentheses: value found with a triplet state quantum yield of 0.33.
[b] Equivalent to $4 \cdot \sqrt{\text{background}}$.

Table 2
Experimental concentration detection limits for AlPcS2 in LC using NIR-LIF detection

Laser	Power (mW)[a]	Repetition rate (Hz)[b]	Ratioing[c]	Detection limit[d] (pM)
Nd:YAG/dye	0.08 ($1.3 \cdot 10^6$)	10 (6)	+	40
Excimer/dye	1.4 ($9.3 \cdot 10^5$)	100 (15)	–	4
Diode	10	CW	–	0.2

[a] In parentheses: peak power in mW.
[b] Between brackets: pulse width in ns.
[c] –: ratioing reveals no or limited improvement; +: significant improvement.
[d] Taken as $S/N = 3$ at maximum output power.

same trend. Hence the theoretical approach provides some insight into the factors that determine the attainable detection limits.

4. Conclusions

Pulsed lasers are less suitable than CW lasers for the trace-level detection of analytes in LC systems, even in the NIR region, where fluorescence background is negligible and Raman scatter is low. The high irradiance provided by pulsed lasers is of limited use. The detection limits for the model compound, AlPcS2, obtained with a CW diode laser, an XeCl-excimer laser and a Nd:YAG laser stand as 1:20:200, in good accordance with theory. Maximum S/N ratios occur at powers far below the available maximum (as low as 0.08 mW or 0.5% of the available power for the Nd:YAG laser). This is not due to flicker noise in the output of the lasers, but to excitation saturation. Time-resolved detection has little practical value, because it is not the background that limits the detection sensitivity.

Appendix

Calculation of the number of photons emitted per analyte molecule in a flowing sample upon excitation with either a pulsed or a CW laser

According to Ref. [3] the number of photons emitted per molecule passing through a flow cell, n_f, is given by:

$$n_f = (Q_f/Q_d)[1 - \exp\{-k_a k_d \tau_{Trans}/(k_a + k_f + k_a k_I/k_T)\}], \quad (4)$$

where Q_f is the fluorescence quantum yield and Q_d the photodestruction quantum yield for the analyte concerned; k_I is the rate constant of intersystem crossing, k_T the rate constant for the decay from the T_1 (triplet excited) to the S_0 (singlet ground) state and k_a the absorption rate constant ($S_0 \rightarrow S_1$), which can be calculated from Eqns. 1 and 2. The rate constant for photodestruction from the first excited singlet state (S_1) is indicated by k_d; τ_{Trans} is the transit time of a molecule through the laser beam, defined as the linear velocity of the eluent divided by the beam diameter. The S_1 population decays to S_0 with a rate constant $k_f = 1/\tau_f$, where τ_f is the fluorescence radiative lifetime.

For the pulsed lasers considered here, the term $k_a k_I/k_T$ can be deleted from Eqn. 4, because a molecule that enters the T_1 state can be considered photodestroyed: the large difference in the duration of the laser pulses and the T_1 state lifetime (< 20 ns and 300 μs, respectively) [2] makes it virtually impossible to return to S_0 before the end of the pulse. Thus, although actual photodestruction is negligible, intersystem

crossing has the same irreversible depleting effect on the S_0 state during a laser pulse.

Because the repetition rate is low (≤ 100 Hz), all molecules will have returned to the ground state before the next pulse. However, excitation of an individual molecule by a second laser pulse does not occur, because of the high flow rate used in the gradient LC separation. As a result Q_d can be replaced by Q_T, the quantum yield of triplet state formation, while k_d can be set equal to k_f or $(Q_T/1 - Q_T)k_f$. Hence Eqn. 4 can be rewritten as:

$$n_f = (Q_f/Q_T)[1 - \exp\{-k_a(Q_T/1 - Q_T)k_f\tau_{Trans}/(k_a + k_f)\}] \quad (5)$$

Eqn. 5 only applies to a system under steady-state conditions, which are not met since the pulse duration is on the same time scale as the processes concerned. For simple pulse shapes the pertinent kinetic equations may be solved analytically; they are, however, rather complicated [7]. As an alternative, computer programs can be used that allow numerical treatment of the problem. In this approach the laser pulse is divided in small time intervals, Δt, and the occupancies of the different molecular states at a particular time, t, are calculated by taking the values at $(t - \Delta t)$ as the starting set. In our case the situation can be simplified by considering any transfer to the triplet state as photodestruction (indicated by state D instead of T_1). This means that the relative number of molecules in the different states at time t (denoted as $[S_0]_t$, $[S_1]_t$ and $[D]_t$) can be calculated from Eqns. 6–8, given below:

$$[S_1]_t = [S_1]_{t-\Delta t} + k_a[S_0]_t\Delta t - k_f[S_1]_t\Delta t - k_d[S_1]_t\Delta t \quad (6)$$

$$[D]_t = [D]_{t-\Delta t} + k_d[S_1]_t\Delta t \quad (7)$$

$$[S_0]_t + [S_1]_t + [D]_t = 1 \quad (8)$$

Eqn. 6 deals with the occupancy of the first excited singlet state as a result of excitation, return to the ground state and transfer to D. Eqn. 7 gives the amount of analyte that is not available for excitation because of either actual photodestruction or transfer from S_1 to a state other than S_0 (in this case T_1) for a period of time that is much longer than the duration of the laser pulse, while Eqn. 8 is obvious. Combining Eqns. 6–8 results in:

$$[S_1]_t = [S_1]_{t-\Delta t} + k_a\Delta t - k_a[S_1]_t\Delta t - k_a[D]_t\Delta t - k_f[S_1]_t\Delta t - k_d[S_1]_t\Delta t \quad (9)$$

which can be rewritten as:

$$[S_1]_t = ([S_1]_{t-\Delta t} + k_a\Delta t - k_a[D]_{t-\Delta t}\Delta t)/(1 + k_a\Delta t + k_f\Delta t + k_d\Delta t + k_ak_d\Delta t^2) \quad (10)$$

To obtain the value of $[S_1]_t$ for a non-square laser pulse shape, the dependence of k_a on time has to be known. To simplify the calculations, we assumed a Gaussian decrease in light intensity during the laser pulse (Figs. 5 and 6). In these intensity distributions, which correspond reasonably well with the actual laser pulse profile (cf. Fig. 1), k_a is defined at different times during the pulse (using a 0.5 ns increment interval). With this information, a computer program loop can evaluate the value of $[S_1]_t$ at any time after the start of the pulse. Integration over the transit time gives n_f:

$$n_f = \int_0^t Q_f k_f [S_1]_t \Delta t \quad (11)$$

The results are visualized in Figs. 5 and 6. On the time scale of 50 ns, utilized in Figs. 5 and 6,

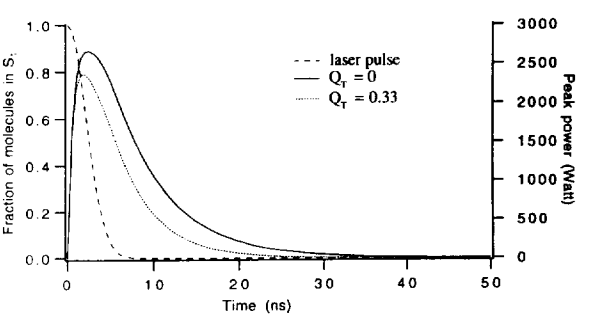

Fig. 5. Computational description of the laser pulse profile for the Nd:YAG laser and the relative number of molecules in the excited state as a result of this pulse, both with (dotted line) and without (solid line) considering transfer to the triplet state ($Q_T = 0.33$ and $Q_T = 0$, respectively). See text for further details.

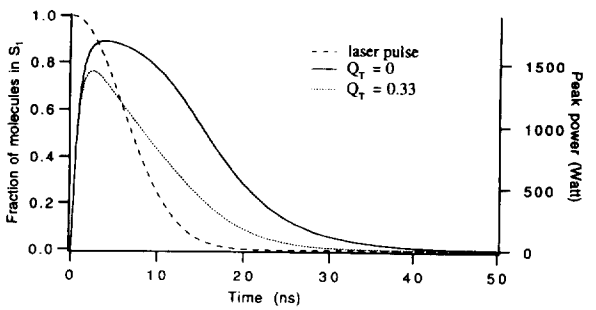

Fig. 6. Computational description of the laser pulse profile for the XeCl-excimer laser and the relative number of molecules in the excited state as a result of this pulse, both with (dotted line) and without (solid line) considering transfer to the triplet state ($Q_T = 0.33$ and $Q_T = 0$, respectively). See text for further details.

the decay of the triplet state is negligible. To show that the influence of a high triplet yield on the number of analyte molecules in S_1 during the laser pulse is rather strong, the curves obtained for $Q_T = 0$ or 0.33 are both given. Their difference will be quantified below.

It should be emphasized that for a CW laser with an average power equal to that of the Nd:YAG or the excimer laser, photodestruction and ground state depletion can be neglected: only a very small and constant fraction of analyte molecules will be in the excited state at any time, for example only 0.01% for the 10 mW 670 nm diode laser. As a result n_f is given by:

$$n_f = Q_f k_f [S_1] \tau_{Trans} \quad (12)$$

where $[S_1]$ represents the steady-state fraction of molecules in the S_1 state:

$$[S_1] = k_a/(k_a + k_f + k_a k_1/k_T)$$
$$= k_a/(k_a + k_f + k_a(Q_T/1 - Q_1)k_f/k_T) \quad (13)$$

The above approach permits a quantitative comparison of the performance of LIF detection set-ups using pulsed and CW lasers as excitation sources. Eqns. 11 (pulsed lasers) and 12 (CW lasers) were used to determine the relative signal (photons s^{-1}) for the 10 mW 670 nm diode laser, the excimer laser and the Nd:YAG laser, utilizing the following parameters: $\epsilon = 180\,000$ l mol^{-1} cm^{-1} at $\lambda = 670$ nm; $Q_f = 0.43$ and $\tau_f = 6$ ns; $Q_T = 0.33$ and $\tau_T = 300$ μs; the beam area is $2.5 \cdot 10^{-3}$ cm^2 for the pulsed lasers and $1.25 \cdot 10^{-3}$ cm^2 for the diode laser. The linear flow rate of the eluent was 1.7 cm s^{-1} (1.0 ml min^{-1}). All lasers were considered under optimal S/N conditions. Using the increment method n_f can be calculated; its value equals 0.6 for the Nd:YAG laser and 1.1 for the excimer laser without photodestruction or transfer to the triplet state ($Q_T = 0$), and 0.4 and 0.6, respectively, for $Q_T = 0.33$. The relative signals in photons s^{-1} (n_f multiplied by the repetition rate of the laser; cf. above) are given in Table 1. Optimum excitation is not achieved at maximum power, since no complete saturation is observed in either Fig. 5 or Fig. 6. At full power for the pulsed lasers, n_f can be calculated to be 3.5 and 8.2, respectively, for $Q_T = 0$, and 1.7 and 2.2 for $Q_T = 0.33$. Clearly, reducing the power more than 100-fold decreases n_f merely 4-fold, if transfer to the triplet state is taken into account. In reality this factor will be even smaller, because of increased photodestruction and ionisation.

The use of a laser that delivers longer pulses will not significantly enhance analyte detectability because of the high triplet state quantum yield. In fact, for an excimer laser delivering 10-fold longer pulses with the same average power, or a similar device delivering a 10-fold higher power within a pulse of normal duration, the signal would be enhanced only 60 and 20%, respectively, for $Q_T = 0.33$. Because the background noise is expected to increase by at least a factor $\sqrt{10}$, detectability will actually deteriorate.

References

[1] A.J.G. Mank, N.H. Velthorst, U.A. Th. Brinkman and C. Gooijer, *J. Chromatogr.* 695 (1995) 165.
[2] A. Beeby, A.W. Parker, M.S.C. Simpson and D. Phillips, *J. Photochem. Photobiol. B. : Biol.*, 16 (1992) 73.
[3] R.A. Mathies, K. Peck and L. Stryer, *Anal. Chem.*, 62 (1990) 1786.
[4] C.M.B. van den Belt, *Ph.D. Thesis*, Leiden University, The Netherlands, 1991.
[5] I. McCubbin, *J. Photochem.*, 34 (1986) 187.
[6] T. Hirschfeld, *Appl. Opt.* 15 (1976) 3135.
[7] I. Carmichael and G.L. Hug, *J. Phys. Chem.*, 89 (1985) 4036.